Spatial structure determination of $(\sqrt{3}\times\sqrt{3})R30°$ and $(1.5\times1.5)R18°$ CO or Cu(111) using angle-resolved photoemission extended fine structure

Edward J. Moler, Scot A. Kellar, W. R. A. Huff, and Zahid Hussain
Advanced Light Source, Lawrence Berkeley National Laboratory, Berkeley, California 94720

Yufeng Chen and David A. Shirley
Departments of Chemistry and Physics, The Pennsylvania State University, University Park, Pennsylvania 16802

(Received 19 June 1996)

We report a study of the spatial structure of $(\sqrt{3}\times\sqrt{3})R30°$ and $(1.5\times1.5)R18°$ CO adsorbed on Cu (111), using the angle-resolved photoemission extended fine structure (ARPEFS) technique. The ARPEFS data were taken along the surface normal-emission direction with a sample temperature of 80 K. The CO molecule adsorbs on an atop site for both adsorption phases. Full multiple-scattering spherical-wave (MSSW) calculations were used to extract the C-Cu bond length and the first Cu-Cu layer spacing for each adsorption phase. The C-Cu bond length is 1.91(1) Å in the $(\sqrt{3}\times\sqrt{3})R30°$ phase and 1.91(2) Å in the $(1.5\times1.5)R18°$ phase. The first layer Cu-Cu spacing is 2.07(3) Å in the $(\sqrt{3}\times\sqrt{3})R30°$ phase. The first layer Cu-Cu spacing in the $(1.5\times1.5)R18°$ phase is 2.01(4) Å, a contraction of 3% from the clean metal value of 2.07 Å. We calculate the bending mode force constant $(1.5\times1.5)R18°$ phase to be $k_\delta=2.2(1)\times10^{-12}$ dyn/cm rad from the above bond lengths combined with previously published infrared absorption frequencies. [S0163-1829(96)07640-0]

I. INTRODUCTION

The adsorption of carbon monoxide on transition-metal surfaces has been extensively studied, both experimentally[1–12] and theoretically,[13–19] with the goal of gaining a basic understanding of the surface chemical bond. Experimentally determined spatial structures of CO adsorbates provide important tests of theoretical models for these systems. We have determined the carbon-copper bond length and the first copper-copper layer spacing for two different, well-ordered coverage phases of CO on Cu(111) using angle-resolved photoemission extended fine structure (ARPEFS).[20]

The adsorption of CO on Cu(111) has been previously investigated with Fourier-transform reflection absorption infrared spectroscopy (FT-RAIRS), electron-energy-loss spectroscopy (EELS), and low-energy electron diffraction (LEED) by Raval *et al.*[8] They found that CO adsorbs on an atop site with the carbon end down for the first two coverage phases, which exhibit a $(\sqrt{3}\times\sqrt{3})R30°$ LEED pattern at ~0.33 ML coverage and a $(1.5\times1.5)R18°$ pattern for a coverage of ~0.44 ML. Based on their observations, they proposed an overlayer structure for the $(1.5\times1.5)R18°$ phase in which there are six CO molecules which each have two adjacent CO adsorbates and one CO which has no adjacently adsorbed molecules. We reproduce this proposed structure in Fig. 1. Additional evidence for the atop adsorption of CO/Cu(111) in the two lower-coverage phases was reported by Hirschmugl *et al.* using far-IR reflection-absorption spectroscopy with synchrotron radiation.[5] They also reported finding a low-frequency vibrational mode which is assigned to a frustrated rotation or bending mode of the Cu-C-O bond in the $(1.5\times1.5)R18°$ phase. The Gibbs free activation energy of desorption was found to exhibit a dramatic rise in transition from the higher coverage $(1.5\times1.5)R18°$ phase to the lower coverage $(\sqrt{3}\times\sqrt{3})R30°$ phase by thermal desorption spectroscopy (TDS).[11] The isosteric heat of adsorption also shows an abrupt change, from ~38 kJ/mole to 50 kJ/mole, at the transition from the $(1.5\times1.5)R18°$ phase to the $(\sqrt{3}\times\sqrt{3})R30°$ phase as determined by surface potential measurements.[6]

The bonding of CO to copper surfaces has been treated theoretically by several workers.[14–19] These investigations infer that the bonding between the CO molecule and the surface are primarily dominated by the donation of the Cu $3d$ and valence electrons into the antibonding $2\pi^*$ molecular orbital (MO), which resides primarily on the carbon atom. Hence, the molecule usually adsorbs with the carbon end down. The transfer of electronic charge to the molecule leads to a positive charge on the metal which stabilizes the repulsive interaction between the occupied 5σ MO and the metal valence electrons.

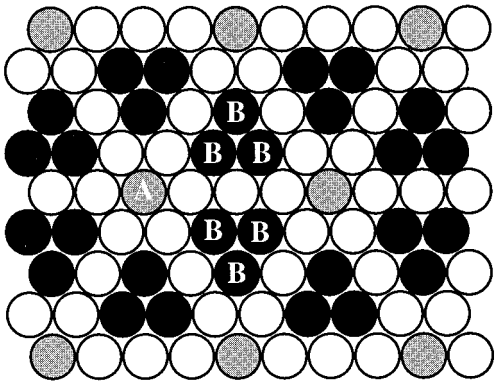

FIG. 1. Adsorption site structure of the $(1.5\times1.5)R18°$ LEED phase proposed by Raval *et al.*[8] The open circles are copper atoms with no CO molecule adsorbed. There are two inequivalent atop adsorption site types labeled *A* and *B* and are shown in gray and black, respectively.

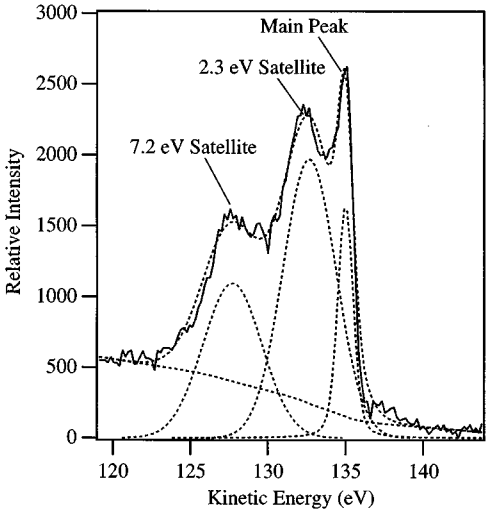

FIG. 2. Typical carbon 1*s* XPS spectrum for this work. The solid line is the experimental data. The dashed lines are the best fit and the deconvolved components.

The x-ray photoelectron spectrum (XPS) of CO on transition-metal surfaces show two strong satellites. The spectrum for CO/Cu(111) shown in Fig. 2 contains satellites at approximately 2.3 and 7.2 eV. These satellites have been interpreted by Tillborg, Nilsson, and Martensson as being due to shakeup transitions between the surface molecular orbitals which occur in a single-step process.[21] This interpretation considers the final state of the remaining electrons to be strongly influenced by the newly created core hole, which pulls the $2\pi^*$-derived surface orbitals below the Fermi level. This state is not an eigenstate of the unperturbed system, leading to a final state which is a sum of the new eigenstates of the adsorbate-plus-core-hole system and thus has significant probability of valence excitations.

The ARPEFS structure determination technique is based on the oscillatory variation in the angle-resolved photoemission intensity from the core levels of near-surface atoms with the electron kinetic energy. It has been successfully used in the past few years to study the local structure of adsorbed atoms and molecules and to determine the substrate layer relaxation.[7,20,22–25] The surface structure can be determined quantitatively by fitting the experimental data with multiple-scattering spherical-wave calculations.[7,20,25,26]

II. EXPERIMENT

The experiments were carried out in an ultrahigh-vacuum chamber with a base pressure $<2\times10^{-10}$ Torr. The chamber was equipped with an ion gun, a four-grid LEED system, a liquid-helium-cooled sample manipulator, and a 50-mm angle-resolving, hemispherical electrostatic electron energy analyzer for x-ray photoemission experiments. The hemispherical analyzer had an acceptance half-angle of approximately 2°.

The copper (111) substrate was cleaned and prepared using the standard UHV surface science techniques of argon-ion sputtering and annealing by *e*-beam heating. The surface order and cleanliness were checked with LEED and synchrotron-radiation excited XPS. There was no detectable

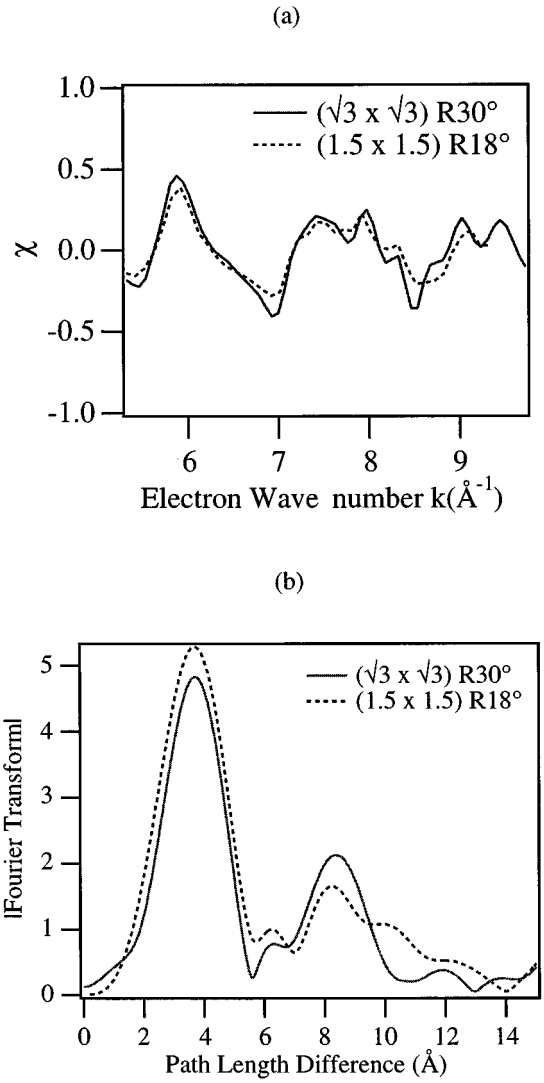

FIG. 3. Experimental carbon 1*s* ARPEFS curves (a) and their Fourier transforms (b) for the two lowest coverage phases of CO/Cu(111). The dominant peaks in (b) at ~3.8 Å and ~8.5 Å are assigned to single-scattering events from the nearest first- and second-layer copper atoms, respectively.

carbon or oxygen contamination on the surface and the LEED showed a sharp 1×1 pattern. The sample was aligned by laser autocollimation and LEED. The sample temperature was measured by a chromel-alumel thermocouple, spot-welded near the sample. A liquid nitrogen reference junction was used with the thermocouple.

The CO overlayers were prepared by first cooling the copper substrate to ~80 K then backfilling the chamber with 1×10^{-8} Torr of CO for ~30 sec through a variable leak valve. The sample was then gently warmed to 130 K at a rate of 0.5 K sec and subsequently cooled to 80 K, resulting in a sharp $(1.5\times1.5)R18°$ LEED pattern. A sharp $(\sqrt{3}\times\sqrt{3})R30°$ pattern resulted from warming the sample to 150 K at the same rate. During the ARPEFS experiments, the sample was maintained at 80 K. We were careful not to damage the overlayers used for the ARPEFS experiment, by checking the LEED pattern only briefly near and the edge of the sample.

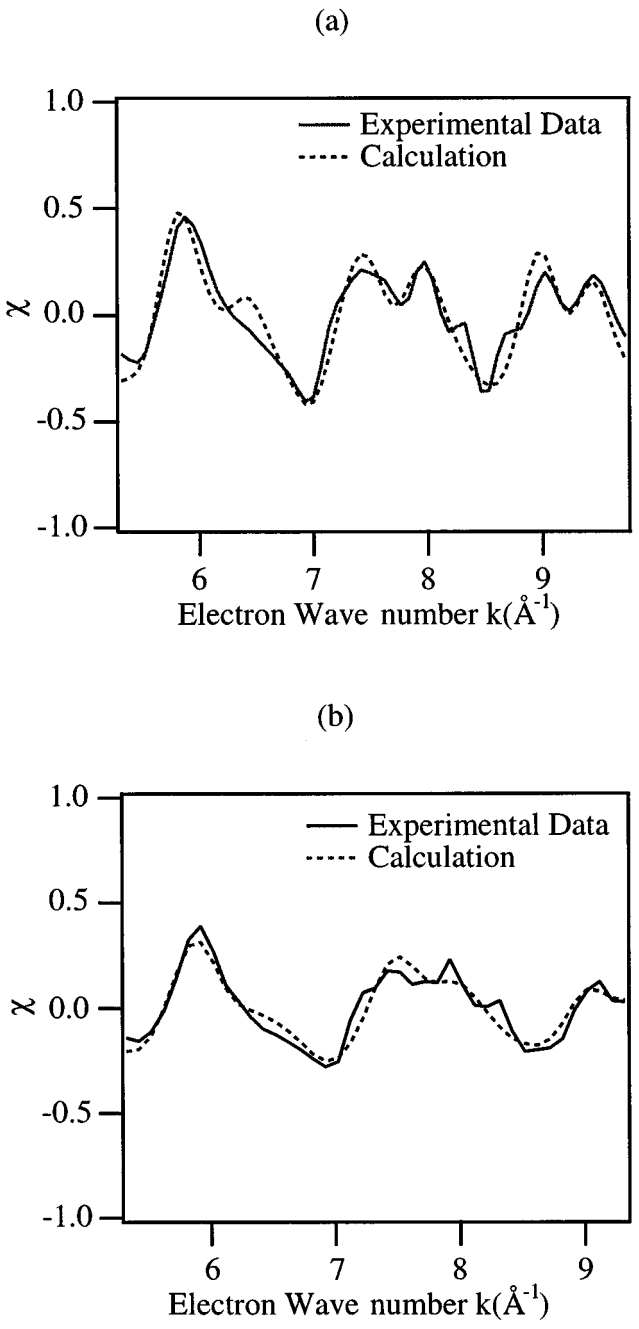

FIG. 4. Comparison of experimental carbon 1*s* ARPEFS curves and MSSW calculations for (a) the $(\sqrt{3}\times\sqrt{3})R30°$ and (b) the $(1.5\times1.5)R18°$ CO/overlayers on Cu(111). The *R* factor between each experimental and calculated curve is 0.12. See text for structural parameters.

The experiments were performed using the spherical-grating x-ray monochromator on beam line 9.3.2 at the Advanced Light Source, Lawrence Berkeley National Laboratory. A 55-m radius, 600-line/mm grating was used to provide photons in the energy range 385–700 eV. The x-ray angle of incidence on the sample was 20° and the photoelectron emission direction was normal to the surface for all experiments. The x-ray monochromator was set to a 0.1% bandpass. The hemispherical electron energy analyzer was set to a resolution of 0.3 eV, yielding an overall resolution of 0.5–0.7 eV.

A series of carbon 1*s* photoemission spectra were taken for each overlayer over a kinetic-energy range of 100–400 eV in electron wave-vector increments of 0.1 Å^{-1}. Figure 2 shows a typical XPS spectrum for this work. The intensities of the main and satellite peaks were determined by a least-squares fitting each peak to a Voigt function, a steplike Voigt-function integral to account for the inelastically scattered electrons associated with the peak, and an experimental background which arises mainly from the inelastically scattered electrons from the substrate. Also shown in Fig. 2 is the deconvoluted components of the spectrum from the best fit. Each peak intensity is normalized to an empirical inelastic background.

The total photoemission intensity $I(k)$, as a function of electron wave number in Å^{-1}, is composed of a slowly varying, atomiclike portion $I_0(k)$ and a rapidly oscillating portion due to the interference of the electron wave resulting from scattering from nearby atoms. The ARPEFS curve $\chi(k)$ is obtained by removing the slowly varying portion

$$\chi(k)=[I(k)-I_0(k)]/I_0(k).$$

$I_0(k)$ is determined by least-square fitting of a low-order polynomial through the experimental curve $I(k)$. Only the main peak intensity was used for the structure analysis. We note here that the satellite peaks show the same ARPEFS oscillations as the main peak, after adjustment to each peak's k value, which is shifted relative to the main peak by the binding energy difference. Further analysis of the satellite-peak ARPEFS for this and other systems will be reported separately.

III. SURFACE STRUCTURE DETERMINATION

The ARPEFS curves for both the $(\sqrt{3}\times\sqrt{3})R30°$ and $(1.5\times1.5)R18°$ overlayers are shown in Fig. 3. Their similarity suggests that the adsorption site is the same for both structures with only small differences in the interlayer spacings, in agreement with previous FT-IR and EELS results which indicate only one kind of adsorption site for these structures.[8] The Fourier transforms of the experimental data are also shown in Fig. 3. The dominant peak at ~4 Å arises from back scattering of the photoelectron from the nearest-neighboring copper atom in the first copper layer. The second peak, at ~8 Å path-length difference, is due to scattering from the nearest second-layer copper atoms.

We have performed full multiple-scattering spherical wave (MSSW) calculations to quantitatively extract the interlayer spacing between the overlayer and substrate and between the near-surface substrate layers. The calculation program is based on the formalism of Rehr and Albers (RA).[26] The RA approximation has been shown to be valid in the energy ranges used in this experiment with second-order (6×6) matrices.[27] The program, developed entirely within our group, is highly optimized for obtaining a best fit to experimental data. It uses second-order matrices (6×6) and up to 8th-order scattering, which produce a convergent calculation at these energies and interatomic distances. The cluster used for the calculations included 97 atoms and was roughly hemispherical in shape with a 7-Å radius about the

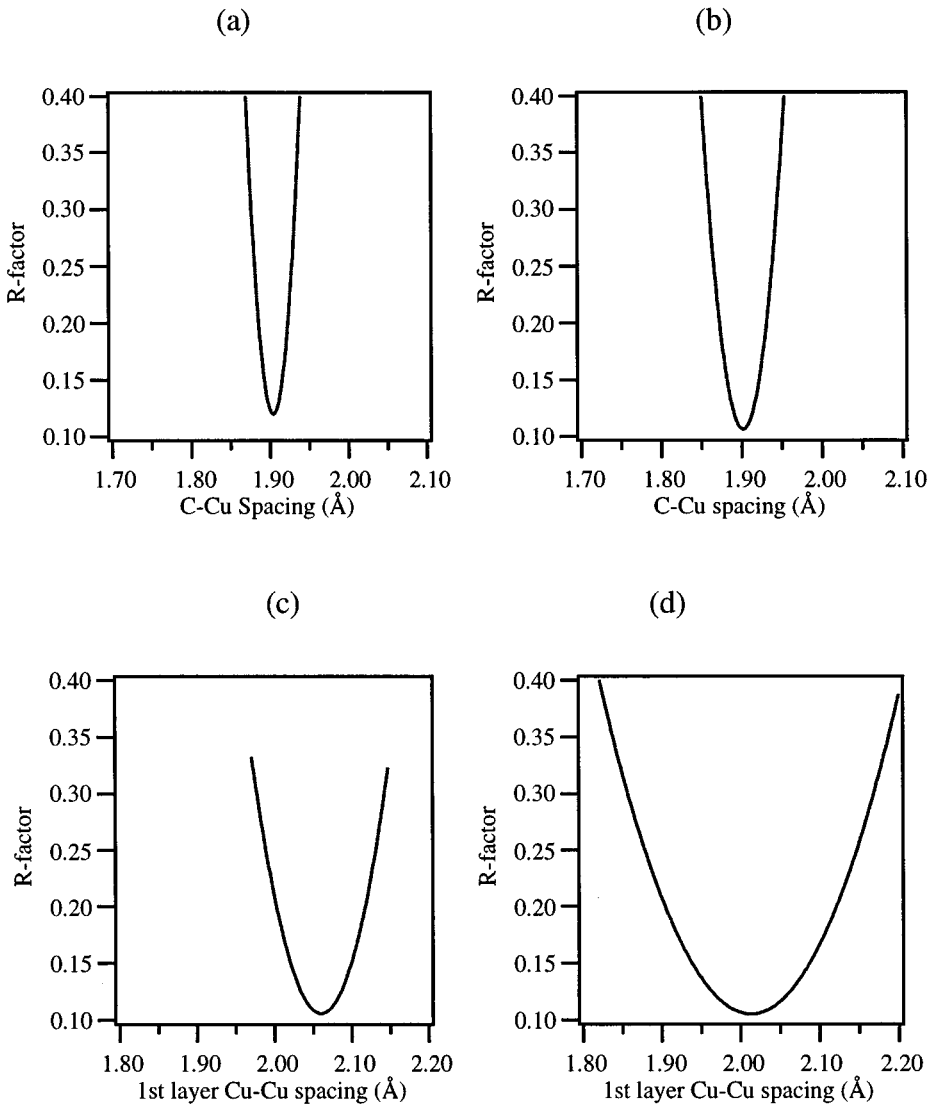

FIG. 5. R-factor curves vs. interlayer spacing. (a) C-Cu spacing for $(\sqrt{3}\times\sqrt{3})R30°$, (b) C-Cu spacing for $(1.5\times1.5)R18°$, (c) first Cu-Cu layer spacing for $(\sqrt{3}\times\sqrt{3})R30°$, (d) first Cu-Cu layer spacing for $(1.5\times1.5)R18°$. The statistical uncertainty of each interlayer spacing is determined from the curvature of the R-factor plot to be ±0.01, ±060.02, ±0.03, and ±0.04 Å for (a), (b), (c), and (d), respectively (see text).

emitting atom. The best fit was defined by the conventional R-factor analysis.[22] Previous studies of these overlayers with FT-IR and EELS determined that the CO molecules adsorbed on atop sites with the carbon end down.[8] We assumed in the calculations that the molecules in the $(1.5\times1.5)R18°$ structure adsorb on nearest atop sites in accordance with the structure proposed by Raval *et al.*[8] The layer spacing between carbon-oxygen, carbon-copper, and between the first three copper layers were allowed to vary. Two nonstructural parameters were also allowed to vary: the surface Debye temperature and the inner potential.

The results of the MSSW calculations with lowest R factor for each structure are shown in Fig. 4. The R factor is 0.12 for both structures. The carbon-copper layer spacing for both structures were found to be the same, 1.91 Å. The first copper-copper layer spacing was found to be 2.07 and 2.01 Å for the $(\sqrt{3}\times\sqrt{3})R30°$ and $(1.5\times1.5)R18°$ overlayer structures, respectively. These derived parameters proved to be insensitive to the C-O bond-length and tilt. This is expected, because the oxygen atom is in a forward-scattering geometry for the normal-emission experiment. We also found the results to be insensitive to neighboring C-O molecules because the amplitude for 90° scattering is very low. The surface Debye temperature was determined to be 200 K. The R factors are relatively insensitive to the inner potential and to the spacing between the second, third, and fourth copper layers.

IV. ERROR ANALYSIS

The statistical uncertainty of each structural parameter is estimated from the curvature of the R-factor plotted versus the parameter value, as previously described method.[25] The uncertainty determined by this method is reported as one standard deviation, i.e., with a 0.67 confidence level.[28] The uncertainty in the last digit appears in parentheses after the number. The R-factor plots for the C-Cu layer spacing and the first Cu-Cu layer spacing are shown for each of the two overlayer structures in Fig. 5. Statistical uncertainties in the C-Cu bond length are 0.01 Å and 0.02 Å for the $(\sqrt{3}\times\sqrt{3})R30°$ and $(1.5\times1.5)R18°$ overlayer structures, respectively. The first Cu-Cu layer spacings have uncertainty estimates of 0.03 Å and 0.04 Å for the $(\sqrt{3}\times\sqrt{3})R30°$ and $(1.5\times1.5)R18°$ overlayer structures, respectively. Possible

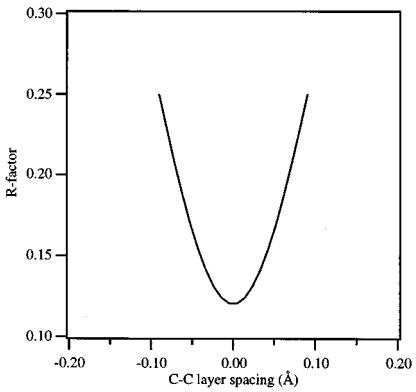

FIG. 6. R-factor vs. interlayer spacing between A-site and B-site carbon atoms (see Fig. 1).

systematic errors for this technique have been previously discussed in detail.[20]

V. FURTHER CONSIDERATIONS CONCERNING THE STRUCTURE OF THE (1.5×1.5)R18° OVERLAYER

The relative positions of adsorbed CO molecules in the (1.5×1.5)R18° overlayer may lead to inequivalent adsorption sites. The question arises as to whether these inequivalent sites may have different layer spacings. As stated above, the normal-emission geometry of this experiment renders the results insensitive to the position of the neighboring CO molecules. We may, however, determine the sensitivity to a variation in layer spacing using R-factor analysis. We have assumed the adsorption structure for the (1.5×1.5)R18° overlayer as proposed by Raval *et al.*,[8] as reproduced in Fig. 1. The A-type adsorption site is one CO molecule with no adjacent adsorbates. The B-type molecules each have two neighboring adsorbates. Note that there are six B-type molecules to one A type. The R factor vs. $A-B$ layer spacing is shown in Fig. 6, in which the B-Cu layer spacing was fixed at 1.91 Å. The R-factor analysis leads to no detectable difference between A-Cu and B-Cu layer spacings, with an uncertainty of ±0.03 Å.

VI. RESULTS AND DISCUSSION

The results of this work are summarized in Table I. The χ curve based on the atop adsorption site of the CO molecule with the carbon end down shows excellent agreement ($R=0.12$) between the MSSW calculations and the experimental data, confirming the previous findings for the two lowest-coverage phases.[5,6,8,11,12] The C-Cu bond length is the same for both coverages, 1.91 Å with uncertainties of ±0.01 Å and ±0.02 Å for the ($\sqrt{3}\times\sqrt{3}$)R30° and (1.5×1.5)R18° overlayer structures, respectively. The C-Cu bond length is similar to the value of 1.8(1) Å for $c(2\times2)$ CO Cu(100) determined by LEED (Ref. 1) with the possible expansion being consistent with the observation that CO is least strongly bound on the (111) face.[29] The first copper-copper layer spacing does not show any change from the clean copper surface spacing of 2.07(2) Å (Ref. 30) for the lower coverage ($\sqrt{3}\times\sqrt{3}$)R30° phase, within experimental uncertainty. There is a distinct contraction of the surface layer for the higher coverage (1.5×1.5)R18° phase to 2.01(4) Å. These experiments were not sensitive to the C-O tilt or bond length.

TABLE I. Summary of bond lengths and layer spacings for two different coverage phases of CO/Cu(111) determined in this work from best fit to MSSW calculations. The statistical errors for the last reported digit are given in parentheses.

LEED structure	C-Cu bond length	First Cu-Cu layer spacing
Clean Cu(111) metal		2.07(2) Å (Ref. 30)
($\sqrt{3}\times\sqrt{3}$) R30°	1.91(1) Å	2.07(3) Å
(1.5×1.5) R18°	1.91(2) Å	2.01(4) Å

The fact that the Cu-C bond length remains constant for both adsorption coverages while the first Cu-Cu layer spacing changes has interesting implications regarding the energetics and dynamics of the two overlayers. The difference in Gibbs free energy between the adsorbed state and the same state activated for desorption has been shown to have a dramatic increase with decreasing coverage between the (1.5×1.5)R18° and the ($\sqrt{3}\times\sqrt{3}$)R30° phases,[11] while the change is less steeply sloped at lower and higher coverages. The coverage-dependent isosteric heat of adsorption also has a significant inflection in the region between the (1.5×1.5)R18° and the ($\sqrt{3}\times\sqrt{3}$)R30° phases, with a nearly constant values of 50 kJ/mole at lower coverages and 38 kJ/mole at higher coverages.[6] The authors of Ref. 6 noted that this inflection could indicate the onset of a different adsorption site, but pointed out that this hypothesis did not explain why the heat of adsorption then remained constant throughout the high coverage region. Subsequent work showed that only atop species exist for these phases.[8] It has also been suggested that competition for back-donated metal d electrons may weaken the Cu-CO bond with increasing coverage.[6] Our results indicate that the Cu-CO bond does not weaken with greater coverage but that the changes in energy of adsorption are related to an adsorbate-induced contraction of the first substrate layer. There is little if any contraction of the first Cu-Cu layer up to a coverage of 0.33 ML. The onset of the inflections in the thermodynamic properties occur at approximately this coverage. The end of the inflections at the 0.44-ML monolayer coverage would suggest that there is no further contraction of the first Cu-Cu layer beyond that determined for the (1.5×1.5)R18° structure.

Theoretical studies of CO on transition-metal surfaces published to date have to our knowledge not specifically investigated the relaxation of the substrate with increasing adsorbate coverage. One notable study has touched upon relevant effects for CO adsorbed on copper (100).[16] Bauschlicher found that two layers are required to describe the binding energy of low coverage CO/Cu(100) convergently and three layers are required at higher coverages.[16] This requirement is ascribed to the repulsion of metal valence electrons by the CO molecules into the second and third copper layers. Bauschlicher also reported that changing the layer spacing of the first two copper layers does not significantly affect the binding energy or geometry of the CO molecule. Our finding of constant Cu–CO bond length, despite the first copper layer contraction, suggests that the binding energy is indeed unchanged. Further theoretical investigation is required to gain an understanding of why a

change in surface coverage of 0.33 ML to 0.44 ML results in a contraction of the first copper layer.

Infrared and electron-energy-loss spectroscopy (EELS) studies of CO/Cu(111) have been previously employed to elicit the dynamics of the adsorbate-substrate interactions.[5,6,8,31] Hirschmugl *et al.*[5] used synchrotron radiation to study the IR absorption region of the Cu-C stretch at 347 cm^{-1}. Their data show no observable shift in the Cu-C stretch mode with increasing coverage, providing further evidence that the Cu-C bond energy is not coverage dependent. However, Hollins and Pritchard found a softening of the C-O bond mode with increasing coverage, using an isotopic-substitution IR technique.[6] In light of our results, it is now clear that, beginning with a coverage of 0.33 ML the first layer Cu-Cu spacing contracts while the C-O bond weakens with increasing coverage, thereby leaving the Cu-C bond largely unchanged.

Hirschmugl, *et al.* observed an IR adsorption band at $\sim$285 cm^{-1} which was assigned to a bending (frustrated rotation) mode of the Cu-C-O complex in the $(1.5\times1.5)R18°$ structure. Calculation of the force constant of the bending-mode vibration, v_2, of a linear molecule requires knowledge of the bond lengths between the atoms. Using our results and the frequency measurements of Hurschmugl, we can determine the bending mode force constant from[5,32]

$$(2\pi v_2)^2=\frac{k_\delta}{l_1^2 l_2^2}\left[\frac{l_1^2}{m_0}+\frac{l_2^2}{m_{\mathrm{Cu}}}+\frac{(l_1+l_2)^2}{m_{\mathrm{C}}}\right], \qquad (1)$$

where k_δ is the force constant, l_1 is the Cu-C bond length, l_2 is the C-O bond length, and m is the mass of each atomic species. We assume the C-O bond length to be that of the gas phase, 1.13(2) Å. This assumption seems justified, as numerous structural studies of CO adsorbed on transition metal surfaces do not find more than 0.02-Å change in bond length, e.g., see Refs. 33 and 34. Additionally, the CO interaction with Cu(111) is among the weakest studied and we feel that the above uncertainty is a rather conservative estimate. The values of the IR absorption frequencies for three isotopes as measured by Hirschmugl *et al.* are 285(8) cm^{-1}, 273(8) cm^{-1}, and 285(6) cm^{-1} for $^{12}C^{16}O$, $^{13}C^{18}O$, and $^{12}C^{18}O$, respectively. Using Eq. (1) above we find the force constant to be $k_\delta=2.2(1)\times10^{-12}$ dyn cm/rad. The uncertainty was estimated by propagation of the experimental uncertainties.[35]

VII. CONCLUSION

We have determined the spatial structure of CO/Cu(111) for two coverages, characterized by $(1.5\times1.5)R18°$ and $(\sqrt{3}\times\sqrt{3})R30°$ LEED patterns, using ARPEFS. The CO molecule adsorbs on an atop site at both coverages with a C-Cu bond length of 1.91 Å, with an uncertainty of ±0.01 Å and ±0.02 Å for the two respective structures. The first Cu-Cu layer spacings were found to be 2.07(3) Å and 2.01(4) Å for the $(1.5\times1.5)R18°$ and $(\sqrt{3}\times\sqrt{3})R30°$ structures, respectively. The bending mode force constants for the Cu-C-O complex in the $(1.5\times1.5)R18°$ structure is calculated from the bond-lengths and published IR absorption frequencies to be $k_\delta=2.2(1)\times10^{-12}$ dyn cm/rad.

ACKNOWLEDGMENTS

We thank the staff and management of the Advanced Light Source at Lawrence Berkeley National Laboratory for their assistance and support with the experimental work. This work was supported by the Director, Office of Energy Research, Office of Basic Energy Sciences, Chemical Sciences Division of the U.S. Department of Energy under Contract No. DE-AC03-76SF00098.

[1] S. Andersson and J. B. Pendry, J. Phys. C **13**, 3547 (1980).
[2] H. Antonsson, A. Nilsson, and N. Martensson, J. Electron Spectrosc. Related Phenomena **54/55**, 601 (1990).
[3] A. M. Baro and H. Ibach, J. Chem. Phys. **71**, 4812 (1979).
[4] J. E. Demuth and D. E. Eastman, Solid State Commun. **18**, 1497 (1976).
[5] C. J. Hirschmugl, G. P. Williams, F. M. Hoffmann, and Y. J. Chabal, J. Electron Spectrosc. Related Phenomena **54/55**, 109 (1990).
[6] P. Hollins and J. Pritchard, Surf. Sci. **89**, 486 (1979).
[7] Z. Huang, Ph.D. Thesis, Department of Chemistry, University of California at Berkeley, 1992.
[8] R. Raval, S. F. Parker, M. E. Pemble, P. Hollins, J. Pritchard, and M. A. Chesters, Surf. Sci. **203**, 353 (1988).
[9] A. Sandell, P. Bennich, A. Nilsson, B. Hernnas, O. Bjorneholm, and N. Martensson, Surf. Sci. **310**, 16 (1994).
[10] A. G. Yodh and H. W. Tom, Phys. Rev. B **45**, 302 (1992).
[11] W. Kirstein, B. Kruger, and F. Theime, Surf. Sci. **176**, 505 (1986).
[12] B. J. Hinch and L. H. Dubois, J. Electron Spectrosc. Related Phenomena, **54/55**, 1990 (1990).
[13] C. Rong and C. Satoko, Surf. Sci. **223**, 101 (1989).
[14] J. Paul and A. Rosen, Phys. Rev. B **26**, 4073 (1982).
[15] A. C. Pavao, M. Braga, C. A. Taft, B. L. Hammond, and W. A. Lester, Phys. Rev. B **43**, 6962 (1991).
[16] C. W. Bauschlicher, J. Chem. Phys. **101**, 3250 (1994).
[17] E. Miyoshi, Y. Sakai, and S. Katsuki, Surf. Sci. **242**, 531 (1991).
[18] M. A. Nygren and P. E. M. Siegbahn, J. Chem. Phys. **96**, 7579 (1992).
[19] R. A. Van Santen, J. Chem. Soc. Faraday Trans. **81**, 1915 (1987).
[20] J. J. Barton, C. C. Bahr, C. C. Robey, Z. Hussain, E. Umbach, and D. A. Shirley, Phys. Rev. B **34**, 3807 (1986).
[21] H. Tillborg, A. Nilsson, and N. Martensson, J. Electron Spectrosc. Related Phenomena **62**, 73 (1993).
[22] J. J. Barton, S. W. Robey, C. C. Bahr, and D. A. Shirley, in *The Structure of Surfaces*, edited by M. A. Van Hove and S. Y. Tong, Springer Series in Surface Sciences Vol. 2 (Springer-Verlag, New York, 1985), pp. 191–198.
[23] S. W. Robey, J. J. Barton, C. C. Bahr, G. Liu, and D. A. Shirley, Phys. Rev. B **35**, 1108 (1987).
[24] K. T. Leung, L. J. Terminello, Z. Hussain, X. S. Zhang, T. Hayashi, and D. A. Shirley, Phys. Rev. B **38**, 8241 (1988).
[25] L. Q. Wang, A. E. Schach von Wittenau, Z. G. Ji, Z. Q. Huang, and D. A. Shirley, Phys. Rev. B **44**, 8241 (1991).
[26] J. Rehr and Albers, Phys. Rev. B **41**, 8139 (1990).
[27] A. P. Kaduwela, D. J. Friedman, and C. S. Fadley, J. Electron

Spectrosc. Related Phenomena **57**, 223 (1991).
[28] W. H. Press, S. A. Teukolsky, W. T. Vertterling, and B. P. Flannery, *Numerical Recipes in C* (Cambridge University Press, New York, 1992).
[29] J. Kessler and F. Thieme, Surf. Sci. **67**, 405 (1977).
[30] J. M. MacLaren, J. B. Pendry, P. J. Rous, D. K. Saldin, G. A. Somorjai, M. A. Van Hove, and D. D. Vvedensky, *Surface Crystallographic Information Service: A Handbook of Surface Structures* (D. Reidel, Boston, 1987).
[31] S. Bao, R. Xu, C. Y. Xu, H. Y. Li, L. Zhu, and Y. B. Xu, Surf. Sci. **271**, 513 (1992).
[32] G. Herzberg, *Molecular Spectra and Molecular Structure II. Infrared and Raman Spectra of Polyatomic Molecules* (Van Nostrand Reinhold Company, New York, 1945).
[33] S. D. Kevan, R. F. Davis, D. H. Rosenblatt, J. G. Tobin, M. G. Mason, D. A. Shirley, C. H. Li, and S. Y. Tong, Phys. Rev. Lett. **46**, 1629 (1981).
[34] Z. Q. Huang, Z. Hussain, W. R. A. Huff, E. J. Moler, and D. A. Shirley, Phys. Rev. B **48**, 1696 (1993).
[35] P. R. Bevington, *Data Reduction and Error Analysis for the Physical Sciences* (McGraw-Hill, San Francisco, 1969).